AJNR

High-b-value Diffusion-weighted MR Imaging of Adult Brain: Image Contrast and Apparent Diffusion Coefficient Map Features

Mark C. DeLano, Thomas G. Cooper, James E. Siebert, Michael J. Potchen and Karthik Kuppusamy

AJNR Am J Neuroradiol 2000, 21 (10) 1830-1836
http://www.ajnr.org/content/21/10/1830

AJNR Am J Neuroradiol 21:1830–1836, November/December 2000

High-b-value Diffusion-weighted MR Imaging of Adult Brain: Image Contrast and Apparent Diffusion Coefficient Map Features

Mark C. DeLano, Thomas G. Cooper, James E. Siebert, Michael J. Potchen, and Karthik Kuppusamy

BACKGROUND AND PURPOSE: **Recent improvements in MR gradient technology allow significant increases in diffusion weighting without prohibitive signal-to-noise degradation. The purpose of our investigation was to establish normative references for the signal intensity characteristics and apparent diffusion coefficient values of the adult brain at high b values.**

METHODS: **Fifty adults underwent diffusion-weighted single-shot spin-echo echo-planar MR imaging. Isotropic diffusion-weighted images were obtained with b values of 0, 1000, 2000, 2500, 3000, and 3500 s/mm^2. Qualitative assessments were made in multiple regions of interest in gray and white matter. Three apparent diffusion coefficient maps were generated for each of six patients with a 2-point technique at a b value of 0 and at b values of 1000, 2000, and 3000 s/mm^2.**

RESULTS: **Increasing b values result in a progressive decrease in the gray to white matter signal intensity ratio. Isointensity between gray and white matter results at b values between 1000 and 2000 s/mm^2. At b values greater than 2000, the gray-white pattern reverses relative to the usual b value of 1000. Apparent diffusion coefficient values were shown to decrease with increasing b values.**

CONCLUSION: **Attention to the reversal of gray-white contrast and the dependence of apparent diffusion coefficient on the b value are important in avoiding erroneous assignment of pathologic abnormalities to normal regions. This study provides the normative data for future diffusion investigations performed at high b values.**

Recent improvements in MR gradient technology allow significant increases in diffusion sensitivity without prohibitive signal-to-noise degradation. Understanding the appearance of images obtained with higher b values is critical for the assessment of future clinical applications and investigations using this technology. The ability of current diffusion-weighted imaging to detect and delineate restricted diffusion is well documented (1–5). The purpose of our investigation was to establish normative standards for the signal intensity characteristics and trace apparent diffusion coefficient (ADC) values of the adult brain at varying high b values.

Received July 23, 1999; accepted after revision May 10, 2000.

From the Michigan State University (M.C.D., T.G.C., J.E.S., M.J.P.), Department of Radiology, East Lansing, MI, and General Electric Medical Systems (K.K.), Waukesha, WI.

Presented at the annual meeting of the American Society of Neuroradiology, San Diego, May 1999.

Address correspondence to Mark C. DeLano, MD, Department of Radiology, 184 Radiology Building, Michigan State University, East Lansing, MI 48824.

Increased gradient amplitudes permit higher b values and greater diffusion sensitivity. Gradient subsystems available on clinical imagers with echo-planar imaging have been limited to diffusion-weighted imaging with b values up to 1200 s/mm^2. Newer clinical imagers can provide b values of 3500 s/mm^2 with echo times less than 100 ms. Isotropic diffusion-weighted images at the standard diffusion gradient strength of 1000 s/mm^2 reveal relative hyperintensity of cortical gray matter compared with white matter. The signal characteristics of adult brain at higher b values have not been reported.

This investigation aimed to establish normative references for the signal intensity characteristics and trace ADC measurements of the adult brain with diffusion-weighted spin-echo echo-planar imaging at varying high b-value diffusion sensitivities. Furthermore, this study provides the normative data for future diffusion investigations performed at high b values.

Methods

Participants

Fifty healthy adults, ranging in age from 17 to 65 years, underwent diffusion-weighted MR imaging. Patients were re-

ferred with complaints of headache and for screening for possible neoplasm or multiple sclerosis. Some served as control participants for various concurrent functional imaging studies. Participants were excluded if underlying pathologic abnormalities were revealed by standard imaging sequences.

Imaging

All images were obtained with a 1.5-T clinical imager optimized for neuroimaging with a 150-T/m/s slew rate and a 40-mT/m maximum gradient strength. Single-shot spin-echo echo-planar imaging isotropic diffusion-weighted images were produced with b values of 0, 1000, 2000, 2500, 3000, and 3500 s/mm^2. Other imaging parameters included 10000/72–96 (TR/TE); field of view, 38 × 19 cm; matrix, 192 × 128; section thickness, 5 mm; section gap, 0 mm; and number of acquisitions, one to four. Higher numbers of acquisitions and minimum echo times were used to improve signal-to-noise ratios at higher b values in 43 of 50 participants. The number of acquisitions was adjusted for each b value: b = 1000 images, number of acquisitions = one; b = 2000 images, number of acquisitions = two; b = 3000 images, number of acquisitions = four.

Quantitative assessment of trace ADC measurements and of signal intensity variation with b-value modulation was conducted for six of the 50 participants using a fixed echo time and variable numbers of excitation. One of the 50 participants was studied with a fixed number of excitations to control for potential influence on the ADC measurement while the echo time was held constant. This participant also underwent imaging with a fixed number of excitations and variable echo times of 96 and 72 ms at a b value of 1000 to assess the effect of echo time modulation on ADC measurement. The ADC data regarding this participant were not averaged with those of the other six because of the differing numbers of excitation.

The signal characteristics of diffusion-weighted imaging sequences were qualitatively assessed for all 50 participants and are reported together because they were independent of the number of signal averages and echo time. In the spin-echo echo-planar diffusion-weighted imaging pulse sequence, the duration of diffusion bipolar gradient pulses and the duration between the two bipolar gradient pulses were held constant for different b values; hence, different b values were obtained by changing the gradient strength of the bipolar gradient pulses while keeping the diffusion time constant.

Data Analysis

Qualitative assessments were made of gray-white contrast and regions of interest (ROI) in the cortical gray matter, centrum semiovale, caudate nuclei, lentiform nuclei, thalami, internal capsules, central pons, middle cerebellar peduncles, and dentate nuclei for isotropic diffusion-weighted images. Quantitative ADC measurements were made from ADC images for the same ROI for six participants.

The diffusion-weighted imaging signal intensity ratio of putamen to centrum semiovale white matter was calculated for b values of 1000, 2000, and 3000 s/mm^2 for the six participants evaluated with a fixed echo time and variable numbers of excitation. Although the signal intensity of putamen is not always isointense to cortical gray matter, the putamen was chosen to avoid the issue of partial volume averaging of CSF in the measurement of gray matter signal intensity. The centrum semiovale is heterogeneous on diffusion-weighted imaging, particularly at higher b values. Therefore, measurements were independently obtained for two areas of white matter that were visually assessed to have the greatest and least signal intensity on the diffusion-weighted images. All measurements were obtained using a developmental software program on a separate workstation.

Image Processing

The isotropic diffusion-weighted images were generated using the cube root of the products of the signal intensities obtained from images sensitized for diffusion along each of the three orthogonal axes (ie, $(I_xI_yI_z)^{1/3}$). Quantitative ADC measurements were made from ADC images created with a two-point linear fit approach. This method involves generating images with two different b values ($b_0 = 0$ and $b_1 = X$ s/mm^2) and then solving the equation for the diffusion coefficient. For the two-point case:

$$D_{apparent} = \ln (S_0/S_1)/(b_1 - b_0) \quad (1)$$

where ln is the natural logarithm, and S_0 and S_1 are the image intensities obtained with b values of b_0 and b_1, respectively. ROI size was 55 mm^2 for all measurements. CSF spaces were avoided to minimize partial volume averaging.

Results

Gray-White Contrast

The pattern of gray-white matter contrast observed on the diffusion-weighted imaging obtained with b values of 1000 s/mm^2 is similar to the contrast features of T2-weighted images, with gray matter hyperintense to white matter. Increasing b values result in progressively greater diffusion weighting while diminishing the appearance of T2 weighting. At b values greater than 2000, the gray-white pattern reverses relative to what is observed at the usual b value of 1000. The most pronounced reversal occurs at a b value of 3500 s/mm^2 (Fig 1). Isointensity between cortical gray and white matter accordingly results at b values between 1000 and 2000 s/mm^2, although the precise value corresponding to isointensity was not determined.

ROI Assessment

Several regions of normal brain are relatively hyperintense on diffusion-weighted imaging performed at lower diffusion gradient strengths. These include the posterior limbs of the internal capsules, the mesial frontal lobe cortex, the central midbrain and pons, and the insular cortex. The degree of hyperintensity in the mesial frontal lobe cortex and the insular cortex was greatest on the diffusion-weighted images obtained with a b value of 1000, gradually becoming isointense with surrounding cortex on images obtained with progressively higher b values (Fig 1). The focal assessment of ROI in subcortical white matter structures revealed the general trends toward hyperintensity on the images obtained with b values greater than 2000 s/mm^2. This was most evident in the subcortical white matter, centrum semiovale, posterior internal capsule, and central brain stem regions exhibiting relative hyperintensity. These signal characteristics were independent of echo time and number of excitations.

Signal intensity ratios provided a quantitative assessment of the gray-white matter contrast on diffusion-weighted images (Table 1). These measurements indicate a decline in the gray-white matter

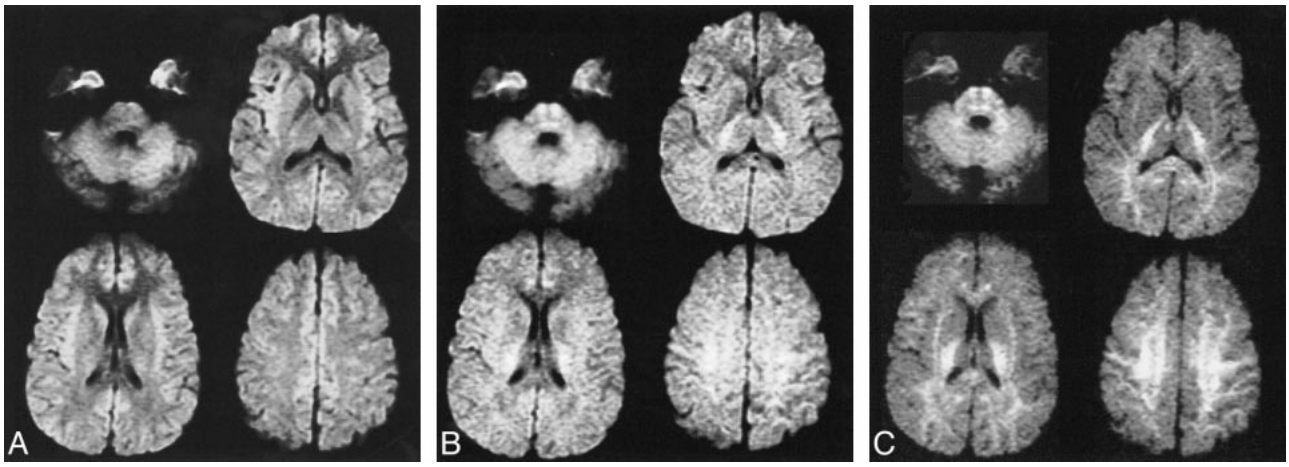

FIG 1. Isotropic diffusion-weighted images with varying b values.

A, Image obtained with a b value of 1000 and 72/1 (TE/excitations). There is hyperintensity of cortical gray matter, particularly in the insular and medial frontal regions.

B, Image obtained with a b value of 2000 and 84/2. Near isointensity of gray and white matter is seen with slight hyperintensity of posterior capsular white matter and pontine regions.

C, Image obtained with a b value of 3500 and 96/4. Progressive hyperintensity of white matter is present with diminished gray matter signal intensity.

TABLE 1: Gray-white matter DWI signal intensity ratios and average values for 6 subjects: fixed TE (96 ms) and variable number of excitations; putamen and centrum semiovale regions of interest were chosen as described in the text

	b = 1000, NEX = 1		b = 2000, NEX = 2		b = 3000, NEX = 4	
Subject	WM Bright	WM Dark	WM Bright	WM Dark	WM Bright	WM Dark
1	0.91	1.15	0.65	0.93	0.48	0.70
2	0.81	1.02	0.63	0.86	0.49	0.71
3	0.88	1.04	0.62	0.92	0.43	0.60
4	0.89	1.12	0.58	0.74	0.50	0.67
5	0.76	1	0.64	0.87	0.42	0.61
6	1	1.13	0.73	0.85	0.50	0.69
Average	0.88	1.08	0.64	0.86	0.47	0.66

Note.—WM bright: ratios obtained from white matter of greatest signal intensity; WM dark: ratios obtained from white matter of least signal intensity.

signal intensity ratio with increasing b values for ROI in the putamen and centrum semiovale white matter.

ADC Measurements

ADC values decreased with increasing diffusion weighting. Greater SDs were noted for ROI adjacent to CSF spaces and for ADC maps derived from the single number of excitations with a b value of 1000 (Fig 2 and Table 2). ADC measurements were shown to vary with diffusion sensitivity, independent of number of excitations (Table 3). Echo time did not affect the mean ADC values measured at a fixed number of excitations (Table 4). Differentiation of gray and white matter on the ADC maps improved with increasing b values (Fig 3).

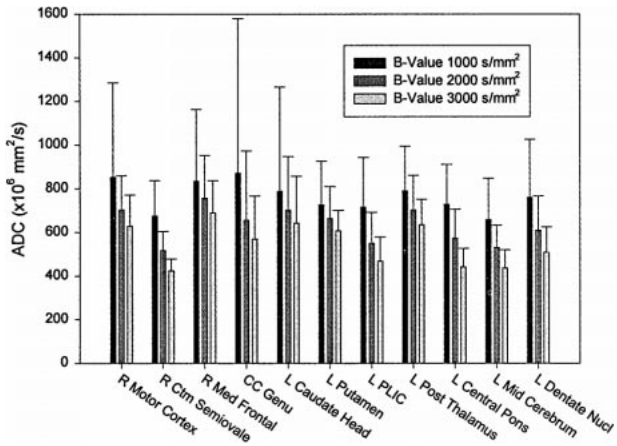

FIG 2. Mean ADC values with SDs for ROI in six participants. Echo time was fixed at 96 ms for all acquisitions. The numbers of excitation were varied to improve signal-to-noise ratios at higher b values: numbers of excitation were one, two, and four for b values of 1000, 2000, and 3000, respectively. ADC values diminish with increasing b values. ADC SDs decrease with multiple numbers of excitaiton.

Discussion

Diffusion imaging at standard b values is a remarkably useful tool in the detection and delineation of restricted diffusion in the clinical setting, particularly in the evaluation of acute ischemia. Understanding the appearance of images obtained at standard and higher b values is critical for the assessment of future clinical applications and investigations using this technology. Our investigation provides normative references for the signal intensity characteristics and ADC values of the adult brain at varying high b-value diffusion sensitivities. The qualitative and quantitative features of diffusion images obtained with varying b values provide an opportunity to gain insight into the

TABLE 2: Mean ADC and SD for six subjects; fixed TE (96 ms) and variable number of excitations

	b = 1000, NEX = 1		b = 2000, NEX = 2		b = 3000, NEX = 4	
Location	ADC	SD	ADC	SD	ADC	SD
R motor cortex	860	359	713	109	625	101
R centrum semiovale	705	111	542	66	445	39
R medial frontal cortex	825	222	726	83	692	94
CC genu	797	294	648	240	594	132
L caudate head	756	254	689	172	622	156
L putamen	712	137	656	86	595	69
L PLIC	720	147	564	94	480	79
L post thalamus	810	146	700	87	637	73
Lat ventricle	2353	1008	1530	321	1247	312
L central pons	807	145	618	94	466	64
L middle cereb ped	699	140	559	75	456	62
L dentate nucleus	780	225	598	127	516	93

Note.—R = right, L = left, CC = corpus callosum, PLIC = posterior limb internal capsule, Post = posterior, Lat = lateral, Cereb Ped = cerebellar peduncle. All values × 10E-6 mm^2/s.

TABLE 3: Mean ADC and SD for single subject: fixed number of excitations (2) and TE (96 ms)

	b = 1000, TE = 96		b = 2000, TE = 96		b = 3000, TE = 96	
ROI Location	ADC	SD	ADC	SD	ADC	SD
R motor cortex	811	220	771	119	668	147
R centrum semiovale	722	66	543	55	475	35
R medial frontal cortex	866	67	724	82	667	71
CC genu	923	323	778	190	576	102
L caudate head	847	336	749	117	661	62
L putamen	717	92	648	47	638	66
L PLIC	679	52	605	52	509	57
L post thalamus	717	112	677	70	649	65
Lat ventricle	2670	403	1780	315	1280	105
L central pons	737	86	583	39	535	74
L middle cereb ped	612	58	511	64	455	44
L dentate nucleus	684	68	663	78	555	50

Note.—R = right, L = left, CC = corpus callosum, PLIC = posterior limb internal capsule, Post = posterior, Lat = lateral, Cereb Ped = cerebellar peduncle. All values × 10E-6 mm^2/s.

TABLE 4: Mean ADC and SD for single subject with fixed number of excitations (2) and variable TE (72 and 96 ms) at b = 1000 s/mm^2

	b = 1000, TE = 96		b = 1000, TE = 72	
ROI Locations	ADC	SD	ADC	SD
R motor cortex	811	220	822	197
R centrum semiovale	722	66	702	58
R medial frontal cortex	866	67	839	79
CC genu	923	323	924	404
L caudate head	847	336	845	222
L putamen	717	92	748	55
L PLIC	679	52	718	66
L post thalamus	717	112	725	98
Lat ventricle	2670	403	3160	281
L central pons	737	86	668	47
L middle cereb ped	612	58	600	51
L dentate nucleus	684	68	712	64

Note.—R = right, L = left, CC = corpus callosum, PLIC = posterior limb internal capsule, Post = posterior, Lat = lateral, Cereb Ped = cerebellar peduncle. All values × 10E-6 mm^2/s.

physiological basis of diffusion imaging as different characteristics of tissue are revealed at different diffusion sensitivities. Increasing the acquisition b value has several implications for diffusion-weighted imaging. The gray-white contrast reversal results in an alteration of the lesion-to-background contrast. The relative conspicuity of restricted diffusion in gray matter is expected to be greater at higher b values, whereas lesion conspicuity in white matter may be greater at lower b values. The optimal b value for evaluation of specific disease states with diffusion-weighted imaging must be determined. The use of multiple sequences with differing b values may yield complementary results (Fig 4).

The pattern of gray-white matter contrast in the diffusion-weighted images obtained with b values of 1000 s/mm^2 is likely a result of the residual T2 weighting. The artifactual hyperintensity or ''T2 shine-through'' seen on diffusion-weighted images of lesions with T2 hyperintensity is also likely a result of the residual T2 weighting present in the

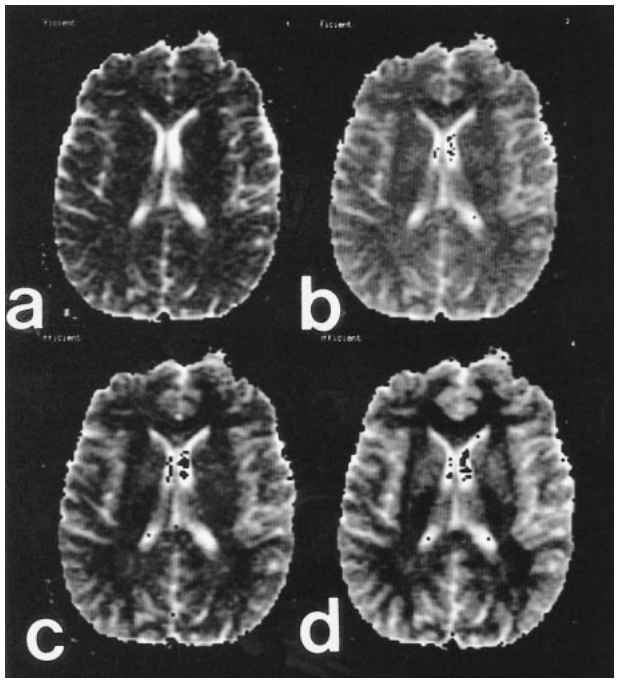

FIG 3. ADC maps at varying b values. Improved gray-white differentiation is noted with increased b value. *A,* b = 1000; *B,* b = 2000; *C,* b = 2500; and *D,* b = 3500.

diffusion trace images. Higher b-value images have relatively less intrinsic T2 weighting and may be useful in differentiating restricted diffusion from T2 shine-through (Fig 4).

The changes in the relative diffusion-weighted imaging signal intensity of gray and white matter with b-value modulation are predicted by the signal intensity equation for a spin-echo diffusion-weighted image, which is given by:

$$S = N(h) \times (1 - \exp(-TR/T1)) \times \exp(-TE/T2) \times \exp(-bD) \qquad (2)$$

assuming monoexponential diffusion, where N(h) is the proton density, TR is the pulse repetition time, T1 is the spin-lattice relaxation time, TE is the spin-echo time, T2 is the spin-spin relaxation time, b is the strength of the diffusion gradient, and D is the diffusion coefficient. Using this equation, we plotted the theoretical signal intensities for gray and white matter by using average imaging parameters and tissue relaxation values (6, 7). From these data, it is possible to derive hypothetical signal intensity curves for a range of b values (Fig 5). The progressive increase in white matter intensity and decrease in gray matter intensity on diffusion-weighted images with increasing b values shown empirically by our data (Fig 1 and Table 1) are predicted by this model.

Table 2 unambiguously shows a consistent pattern of decreasing ADC measurements for increasing b values. For some ROI, the ADC decreased approximately 30% to 35% between b values of 1000 and 3000 s/mm^2. These data indicate that the

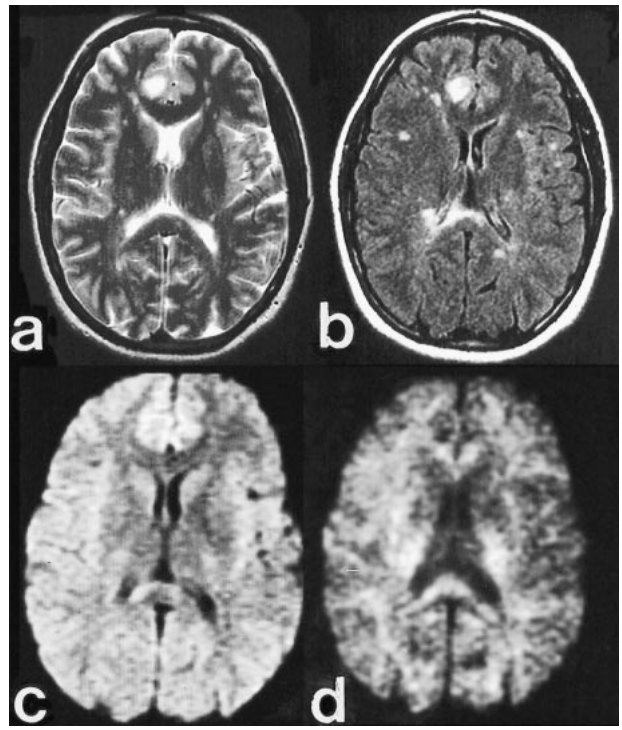

FIG 4. Clinical case of multiple sclerosis.

A, Fast spin-echo axial T2-weighted image (4000/102/2 [TR/TE/excitations]) shows a dominant subcortical right cingulate gyrus lesion with marked hyperintensity.

B, Fast-FLAIR image (10000/145/2200/1 [TR/TE/excitations]) highlights additional subcortical and periventricular plaques, including a large lesion in the right side of the splenium.

C, Diffusion-weighted image (10000/72/1) obtained with b = 1000 s/mm^2 reveals slight hyperintensity in the right cingulate lesion, similar to the contralateral mesial frontal region, and hyperintensity in the right splenium lesion.

D, Diffusion-weighted image (10000/96/1) obtained with b = 3500 s/mm^2 reveals marked hypointensity in the right cingulate lesion, likely reflecting reduced T2 weighting and less T2 shine-through. Persistent hyperintensity in the right splenium lesion is likely due to the normal anisotropy of the splenium and inconspicuity of hypointense lesions adjacent to the CSF spaces. This emphasizes the complementary relationship of the diffusion-weighted acquisitions obtained at standard and high b values.

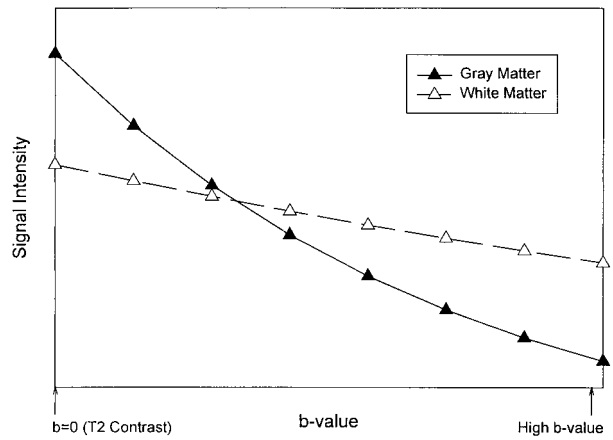

FIG 5. Reversal of gray-white matter contrast with increasing b values. Relative signal intensity values obtained from equation 2 in the text.

monoexponential assumption underlying these calculations is inappropriate. If this assumption were valid, as the b values increased, the ADC would remain constant for all calculations. A likely explanation of these data is that the apparent diffusion is more accurately represented by a biexponential response. Rapidly decaying and slowly decaying diffusion components have been described in both animal and human models (8–10). At relatively low b values, signal intensity in the trace images is dominated by a fast diffusion component, D_{fast}, whereas at higher b values, signal intensity is contributed largely by the slower component of diffusion, D_{slow}. Consequently, as b values are increased from 1000 to 3000 s/mm^2, the signal intensity in the trace images transitions from a D_{fast} to a D_{slow} weighting. There are also important differences between intracellular (D_{in}) and extracellular (D_{ex}) diffusion coefficients corresponding to the slow and fast diffusion components, respectively. Niendorf et al (9) showed that the D_{fast} and D_{slow} do not equal but are proportional to D_{in} and D_{ex}, respectively. Kraemer et al (10) showed that the extracellular component dominates at b values less than 1000s/mm^2 and that the ADC measurements obtained at these values primarily reflect extracellular diffusion, especially when the data are fitted to a single exponential.

A multi-component diffusion model has substantial implications for the postprocessing of diffusion trace (ADC) images. Obviously, the two-point calculation is inadequate to characterize the signal intensity as the b value is modulated. The least-squares multi-point approach, although possibly reducing the SD of the measurements, will yield incorrect results. A more sophisticated postprocessing approach is required for these data that uses the biexponential nature of the signal attenuation. One processing avenue to pursue is the non-negative least-squares algorithm that theoretically would extract all diffusion components. However, it is likely that this would require increased b-value sampling density as well as higher b values to improve the resolution of the diffusion measurements. At the very least, this technique would significantly increase the acquisition time necessary to generate the data sets for these calculations.

Burdette et al (11) compared ADC measurements using two-point and six-point techniques in the b-value range of 0 to 1000 s/mm^2 and noted that the mean percentage difference between the two methods was 0.84%. Their results support the concept that the ADC calculation for a two-point calculation is practical, reproducible, and acceptable for clinical diffusion examinations. We observed significant variation in the ADC value for b values of 1000 to 3000 s/mm^2, well beyond the range that was investigated by Burdette et al. For practical purposes, our results suggest that it is not valid to extrapolate ADC values obtained at a particular b value to other b values.

The large SDs of the ADC measurements, particularly at ROI near CSF spaces, result in some overlap in ADC values for normal gray and white matter structures. This may impact the quantitative values of the ADC measurements in routine clinical imaging. The decrease in SDs with increasing b values for the six participants averaged in Table 2 was likely a result of signal averaging. The SDs for the participant for whom a fixed number of excitations was used were not b-value-dependent (Table 3). Increasing numbers of excitation and careful ROI placement may reduce the SDs of ADC measurements. ADC measurement was not affected by echo time modulation in the single participant evaluated (Table 4).

Ulug et al (12) addressed the problem of ADC reproducibility within and between neuroanatomic sites. The relatively large SDs of ADC measurements observed in this study again emphasize this issue. The results presented by Ulug et al showed minimal interparticipant variation when comparing ipsilateral to contralateral ratios of ADC as a means to quantitate changes in ADC measurements.

The usefulness of ADC maps has been questioned by other investigators who cite a greater sensitivity and accuracy and a very high specificity in the detection of early cerebral infarctions (98.1, 97.7, and 97.1%, respectively) for orthogonal axis diffusion-weighted images compared with ADC maps (13, 14). The validation of their conclusions in the evaluation of stroke at higher b values is necessary. The need for postprocessing, specifically ADC map generation, may be less at higher b values as the intrinsic diffusion sensitivity is increased and the T2 effects are reduced.

The variation in the echo time and the number of signal averages between and within the various subgroups of participants in this study could be considered a limitation of this investigation. The inclusion of participant data obtained with these variations has both positive and negative effects. The qualitative observations regarding signal intensity features were correct for all patients independent of these variations, thus increasing the likelihood of reproducibility by other centers. Conversely, the variations in protocol limited the number of examinations available for quantitative assessment of ADC variation independent of echo time and number of excitations. Measurements were obtained from six participants with a fixed echo time. Averaging of a larger number of participants' data may provide a more reliable standard of reference for normal ADC values.

Conclusion

Interpretation of diffusion-weighted images obtained with b values greater than 1000 s/mm^2 must consider the increasing contribution of diffusion weighting and the diminished T2 effects. Diffusion-weighted images obtained at b values greater than 2000 s/mm^2 have contrast features more ac-

curately reflecting the relative ADC values of gray and white matter, with hyperintensity corresponding to lower ADC values. Restricted diffusion and lower ADC values in white matter results in hyperintensity relative to gray matter on the more heavily diffusion-weighted images. ADC dependence on b value must be considered in the interpretation of these quantitative measurements. Our data indicate that diffusion in human brain is not monoexponential. Although ADC algorithms using the monoexponential assumption are practical, a more complex approach is required to extract the fast and slow diffusion components present in brain tissue. Attention to these findings, especially the reversal of gray-white contrast and ADC dependence on b value, is important in avoiding erroneous assignment of pathologic abnormalities to normal regions. Future studies are necessary to define the role of high b-value diffusion imaging further in the evaluation of acute stroke and other pathologic abnormalities.

Acknowledgments

This work was supported in part by General Electric Medical Systems, Milwaukee, WI.

References

1. Le Bihan D, Breton E, Lallemand D, Grenier P, Cabanis E, Laval-Jeantet M. **MR imaging of intravoxel incoherent motions: application to diffusion and perfusion in neurologic disorders.** *Radiology* 1986;161:401–407
2. Warach S, Chien D, Li W, Ronthal M, Edelman RR. **Fast magnetic resonance diffusion-weighted imaging of acute human stroke.** *Neurology* 1992;42:1717–1723
3. Chien D, Kwong KK, Gress DR, Buonanno FS, Buxton RB, Rosen BR. **MR diffusion imaging of cerebral infarction in humans.** *AJNR Am J Neuroradiol* 1992;13:1097–1102
4. Yuh WT, Crain MR, Loes DJ, Greene GM, Ryals TJ, Sato Y. **MR imaging of cerebral ischemia: findings in the first 24 hours.** *AJNR Am J Neuroradiol* 1991;12:621–629
5. Lovblad KO, Baird AE, Schlaug G, et al. **Ischemic lesion volumes in acute stroke by diffusion-weighted magnetic resonance imaging correlate with clinical outcome.** *Ann Neurol* 1997;42:164–170
6. Le Bihan D, Turner R, Patronas N. **Imaging in brain and tumors.** In: Lebihan D, ed. Diffusion and Perfusion Magnetic Resonance Imaging: Applications to Functional MRI. New York: Raven Press;1995;:134–139
7. Hendrick RE. **Image contrast and noise.** In: Stark DD, Bradley WG, eds. *Magnetic Resonance Imaging*. 3 ed. St. Louis: Mosby; 1999;:43–67
8. Kwong KK, Chesler DA, Baker JR, et al. **Functional magnetic resonance imaging: MR movie of human brain activity.** Presented at the Functional MRI of the Brain Workshop of the Society of Magnetic Resonance in Medicine and the Society for Magnetic Resonance Imaging, Arlington, June 1993
9. Niendorf T, Dijkhuizen RM, Norris DG, van Lookeren Campagne M, Nicolay K. **Biexponential diffusion attenuation in various states of brain tissue: implications for diffusion-weighted imaging.** *MRM* 1996;36:847–857
10. Kraemer F, Darquie A, Clark CA, LeBihan D. **Separation of two diffusion compartments in the human brain.** Presented at the Meeting of the International Society for Magnetic Resonance in Medicine, Philadelphia, May 1999
11. Burdette JH, Elster AD, Ricci PE. **Calculation of apparent diffusion coefficients (ADCs) in brain using two-point and six-point methods.** *J Comput Assist Tomogr* 1998;22:792–794
12. Ulug AM, Beauchamp N Jr, Bryan RN, van Zijl PC. **Absolute quantitation of diffusion constants in human stroke.** *Stroke* 1997;28:483–490
13. Chong J, Lu D, Aragao F, et al. **Diffusion-weighted MR of acute cerebral infarction: comparison of data processing methods.** *AJNR Am J Neuroradiol* 1998;19:1733–1739